Impact of pH levels on the morphological, dielectric and impedance spectral behaviour of cobalt oxide nanomaterials

S. Senthil[a,*], V. Ratchagar[b], T. Thangeeswari[c], S. Srinivasan[d], R. Murugan[e]
[a]*Department of Physics, Chennai Institute of Technology, Chennai – 600 069, Tamil Nadu, India*
[b]*Department of Physics, St. Peter's College of Engineering and Technology, Chennai – 600 054, Tamil Nadu, India*
[c]*Department of Physics, Vel Tech Multi Tech Engineering College, Chennai-600 062, Tamil Nadu, India*
[d]*Department of Physics, Presidency College, Chennai – 600 005, Tamil Nadu, India*
[e]*Department of EEE, St. Peter's College of Engineering and Technology, Chennai – 600 054, Tamil Nadu, India*

Pure Co_3O_4 nanomaterials were synthesized by using Sol-Gel technique at various pH levels (7, 8 and 9). Morphological and structural analysis was done by X-ray diffraction method (XRD), scanning electron microscope (SEM) and energy-dispersive spectroscopy EDX. The X-ray diffraction patterns revealed that the prepared samples crystallized in a cubic structure without any impurities. SEM micrographs validated the influence of pH in altering the morphology of the synthesized compound. The elemental spectrum analysis EDX confirms the presence of cobalt and oxygen without any impurities. Variation of dielectric constant, dielectric loss and impedance were analyzed for various temperatures and different pH values. Dielectric loss value increases at high temperature due to the thermal disturbance of the atoms. Cole-Cole impedance plot gives the information about grain and grain boundaries. DC electrical conductivity values of Co_3O_4 nanomaterials in the temperature range 40ºC to 250ºC increases with increase in pH level from 7 to 9. Arrhenius plot of Co_3O_4 nanoparticles confirmed that the activation energy at various temperature increases with increase in pH levels upto 8, then decreases for pH level 9.

1. Introduction

The nano-sized semiconducting compounds have piqued a large-scale interest in the current years owing to their structural, chemical, physical, nonlinear optical, and magnetic properties which differ from those of their bulk counterparts [1,2]. Metal oxide nanoparticles have a unique property with more photocatalytic efficiency due to their high stability and tunable bandgap [3]. One among them is the cubic spinel structured, cobalt oxide (Co_3O_4), which is a semiconductor material, with its magnetic moment aligned in the anti-ferromagnetic ordering [4-6]. The above-mentioned properties have a great influence on device applications such as gas sensors, information storage components, lithium-ion batteries, environmental-decontaminant catalysts, and solar panel absorbents [7-9]. Co_3O_4 nanoparticles show the good adsorption property of various dyes in water treatment and industrial waste removal applications [10] In the current scenario, the magnetic materials have many gripping characteristics which are convenient for humankind on our everyday basis which comprises of compact-disks, credit card chips, speaker components, instant coolers, fully-automatic doors, etc, Thereby, splendid initiatives have been directed towards the synthesis and enumeration of properties of Co_3O_4 nanostructures [11].

The usage of Co_3O_4 nanoparticles in various applications is depending on their structural, morphological nature and surface area which attains from suitable synthesis methods. Co_3O_4 nanoparticles fabricate by various processes such as chemical precipitation, co-precipitation, dip coating technique, and sol-gel method [12, 13]. Among the various synthesis methods, the sol-gel method is less in cost, more efficient to produce controlled nanosized material, has no need for difficult instruments, and gives high-purity samples and a fast process [14, 15].

Further, the various parameters such as particle size, temperature, pH level, the concentration of the precursors, and porosity affect the optical, magnetic, dielectric, and photocatalytic properties of Co_3O_4 nanoparticles [16]. Abdallah and Awad's research results confirm that the magnetization value of Co_3O_4 nanoparticles depends on the synthesis process and particle size. Moreover, it confirms the dielectric properties also depend on temperature [17]. pH level affects the shape of the synthesized nanoparticle. Also, the temperature and capping element also affects the crystallinity and shape of the nanoparticles [18, 19]. Lattice parameters a and c values also get affected by the pH level of synthesized samples [20]. A pH value not only affects the structural and morphology of the samples, but it also affects the dielectric properties also. In $CaCu_3Ti_4O_{12}$ ceramics, the dielectric loss is reduced by tuning the ph value of the precursor solution [21]. Repulsive and attractive forces between particles and substrate affect the particle coverage. Particle coverage is tuned by pH value, if the pH level increases; the particle coverage gets drastically decreased. By tuning the particle coverage we can use the synthesized material in biological sensors [22]. Optical transmission value, count of crystallites per unit area, and thickness of thin films depend on the pH level of the synthesized sample [23].

In this research work, we have reported the structural, morphological, impedance spectral analysis, and dielectric properties of Co_3O_4 nanomaterials prepared by the sol-gel method under different pH levels.

2. Experimental procedure

2.1. Material synthesis

The sample is synthesized by a simple and low-cost sol-gel method. Analytical grade of cobalt chloride hexahydrate and ammonia hydroxide solution with a purity of 99.9% from Merck are used in this research work as precursor samples without further purification process. Initially, 0.1 mol of cobalt chloride hexahydrate is added to 50 ml of demineralised water and 20 ml of ammonium hydroxide solution was added to 30 ml of double distilled water. Later both the solutions are mixed and magnetically stirred well for 6hrs at room temperature. The pH of the solution was maintained by the addition of ammonia (NH_4) solution. The obtained green precipitate is washed using ethanol 10 times and later washed with double distilled water. Then the precipitate is dried at $80^{\circ}C$ for 12 hrs in a hot air oven to remove water content and calcined at $500^{\circ}C$ for 5 hrs to obtain a sample in powder form. The material was synthesized by maintaining various pH levels of the reaction solution at 7, 8 and 9 respectively.

2.2 Characterization System

Crystalline nature of Co_3O_4 nanomaterials prepared by sol-gel method under different pH levels were studied by X-ray diffraction using Cu Kα radiation (λ=1.5406Å) with the scanning rate of $0.05°s^{-1}$ in the 2θ range from 20° to 80° (BRUKER USA D8 Advance, Davinci. Morphology of the prepared nanoparticles was investigated by Scanning Electron Microscopy (SEM, Hitachi S-3000N, Tokyo, Japan, 0.3 - 30kV). Dielectric studies were carried out with Multi-Channel Battery Cycler System- Won A Tech battery cycler, WBCS3000K8 with Impedance Analyzer.

3. Results and discussion

3.1. XRD Analysis

XRD patterns of the synthesized Co_3O_4 nanoparticles as shown in Figure 1. All diffraction peaks were indexed as (220), (311), (222), (400), (422), (511), (440), (533) lattice planes and well coincided with the JCPDS data (# 78-1970) [5]. Diffraction peaks confirmed that there were no additional impurity peaks. The synthesized material possessed a cubic spinel structure with a space group Fd_3m. It can be observed from the pattern that the intensity of the pattern increases with increasing pH values. Diffraction peaks are broadened with the increase of pH values which attributes to the increase in micro strain shown in Table 1 [1]. On the other side, the broadened diffraction peak in all three pH levels confirmed the crystallite size of the synthesized nanoparticle is small [9]. The crystallite size was calculated from Scherrer's formula from equation 1 [24,25].

$$D = 0.89\lambda/\beta\cos\theta \qquad (1)$$

where D is the crystal size, λ is the X-ray wavelength, (CuK_α - 1.5406 Å), β is the full width at half maximum of the diffraction peak, and θ is the Bragg diffraction angle of corresponding peaks. It was observed that the crystallite size gets reduced in the range of 10-14 nm with increase in pH level for (311) diffraction plane which is mentioned in table 1.

From Figure 2, it was noticed that the diffraction peak shifted slightly to the right for the pH value 8 and further increased to pH value 9, and then the peak shifted to the left. This shift may be due to the different pH of the reaction solution providing energy to molecules. Molecules in proper equilibrium sites after gaining energy result in the improvement in crystalline and degree of orientation of the Co_3O_4 nanoparticles. Change in peak position may correspond to the crystal defects due to a change in the pH of the sample [14]. The strain was calculated using the Williamson-Hall method as given in equation 2.

$$\beta\cos\theta = \frac{K\lambda}{D} + 4\varepsilon\sin\theta \qquad (2)$$

where,   D = Crystallite size (nm),
           λ = Wavelength (1.5406 Å),
           β = Full width half maximum (FWHM),
           θ = Peak positions and
           ε = Micro strain.

Figure 3 shows the W-H plot of all the prepared samples plotted between $4\sin\theta$hkl and $\beta\cos\theta$ hkl. The calculated strain values were given in Table 1. Figure 3 shows that the pH increases with an increase in the strain value. It was indicated that the lattice expansion which leads to micro strain is enriched in smaller crystal-size particles with an increase in the pH level of the sample. Further, dislocation density and the number of crystallites were estimated by the formula

Dislocation density (δ) = $1/D^2$

Number of crystallites (N) = $1/D^3$

Calculated values were mentioned in the table 1. It is observed that the dislocation density and number of crystallites per unit area values increases with increase in pH value [23].

Table 1. Micro Structural Parameters of Co3O4 nanoparticles.

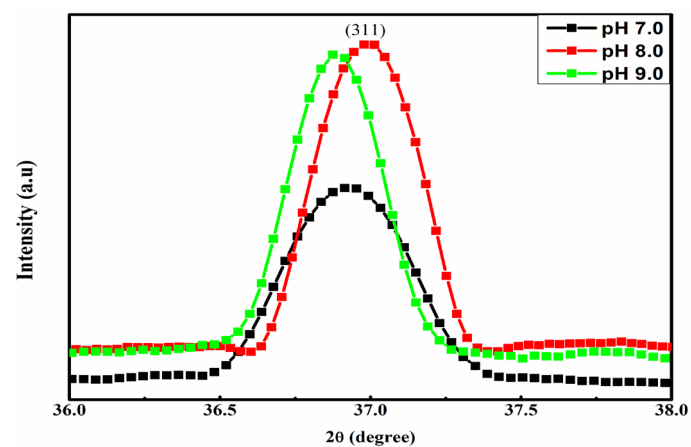| S.No	pH	Crystal Size (nm)	Micro strain (10^{-3})	Dislocation density (δ) $\times 10^{15}$ Lines/m^2	Number of crystallites (N) $\times 10^{23}$
1.	7.0	14	0.072	5.1	3.6
2.	8.0	12	0.205	6.9	5.7
3.	9.0	10	0.549	10	10
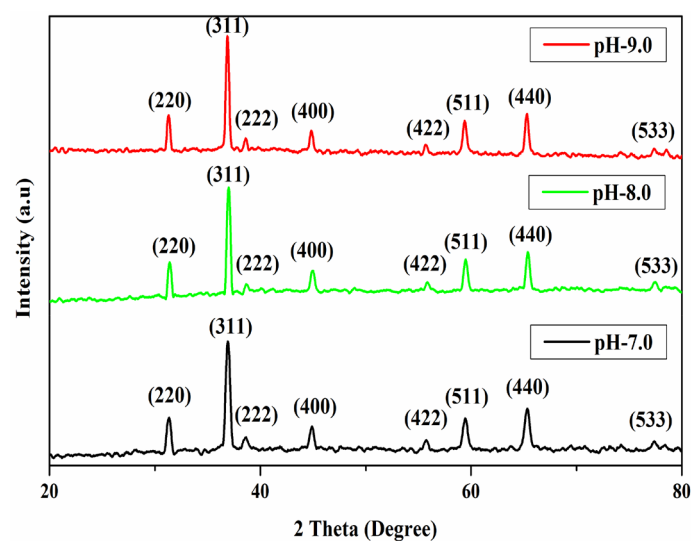
Fig. 1. XRD pattern Co$_3$O$_4$ nanoparticles.
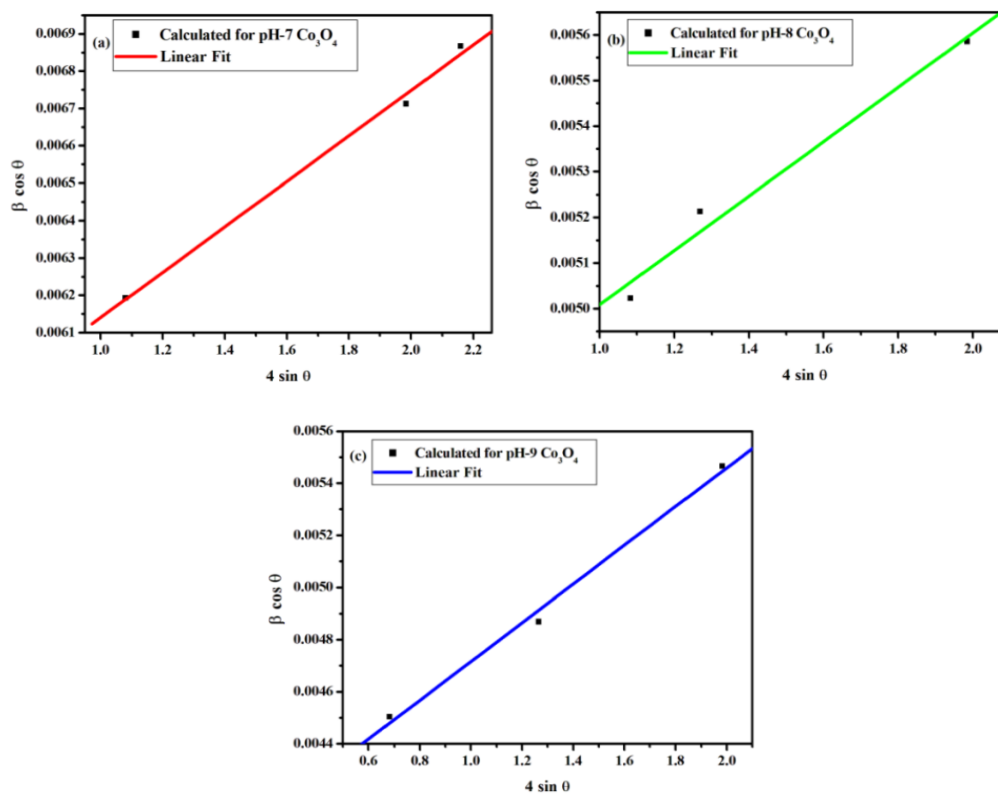

Fig. 2. Peak shifting at different pH levels.

Fig. 3. W-H graph, strain of different pH of Cobalt Oxide nanoparticles.

3.2. SEM & EDX Analysis

The morphology of the prepared samples was analyzed with the help of SEM micrographs. Figure 4 (a) shows the SEM images of cobalt oxide nanomaterials. The figure shows the clear details that the particles are in uniform size and well-defined spherical shapes. Moreover, when the pH of the reaction solution was increased, the shapes of the particles growing in a certain direction (i.e.) sphere to the regular shape of the cubic structure in Fig 4 (b) and Fig 4 (c) shows that the particles of flower shape. Here, the pH of the reaction solution plays a major role in the formation of the nucleation sites which determine the shape of the particles. The other reason for such morphological change might be due to the presence of OH- ions in the precursor solution that creates non-bonding interaction. This intermolecular interaction during the reaction is often referred to as the steric effect, which leads to the rise of repulsive forces between overlapping electron clouds. So it authenticates the transformation from spherical to cubic to agglomerated shape. Fig 4 (a-c) presents the EDX spectrum of the synthesized Co_3O_4 nanomaterials. The elemental spectrum confirms the presence of cobalt and oxygen at appropriate ratios. The absence of any undesired elemental composition ascertains the purity of the samples. It shows the synthesized cobalt is highly pure with no secondary compounds or excess precursors.
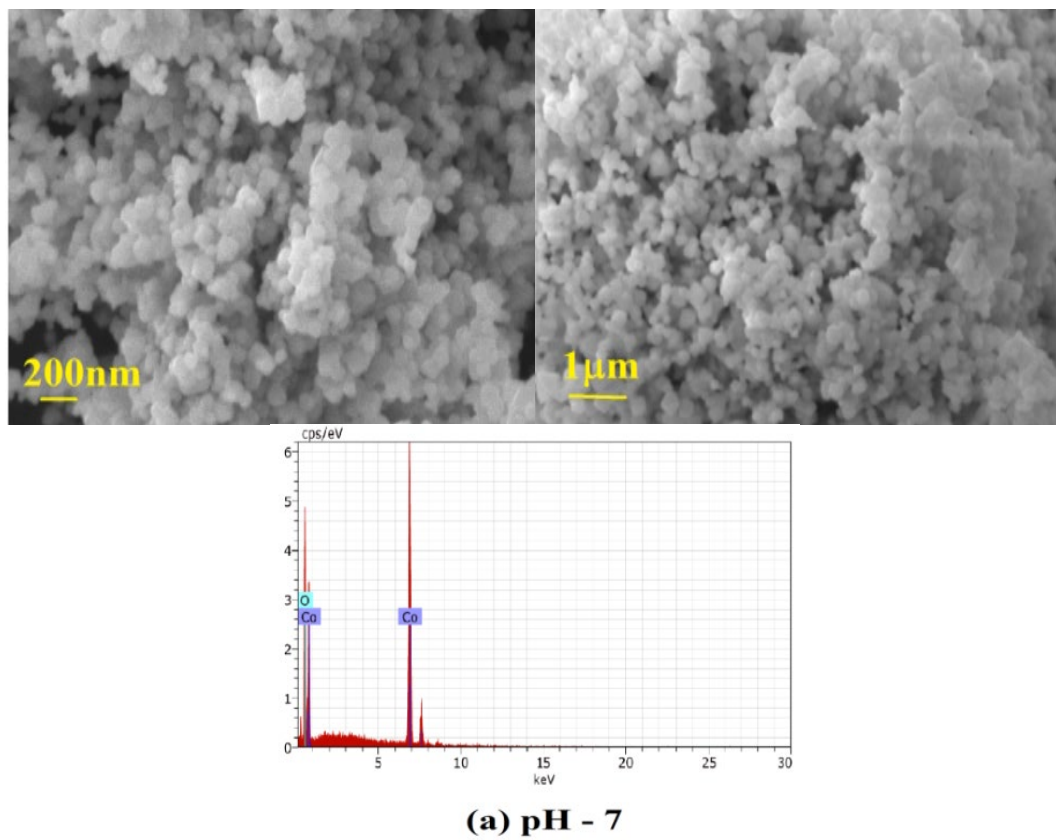
Fig. 4. (a) SEM Image of Co3O4 nanoparticles and EDX Spectrum of Co3O4 nanoparticles (pH=7.0).
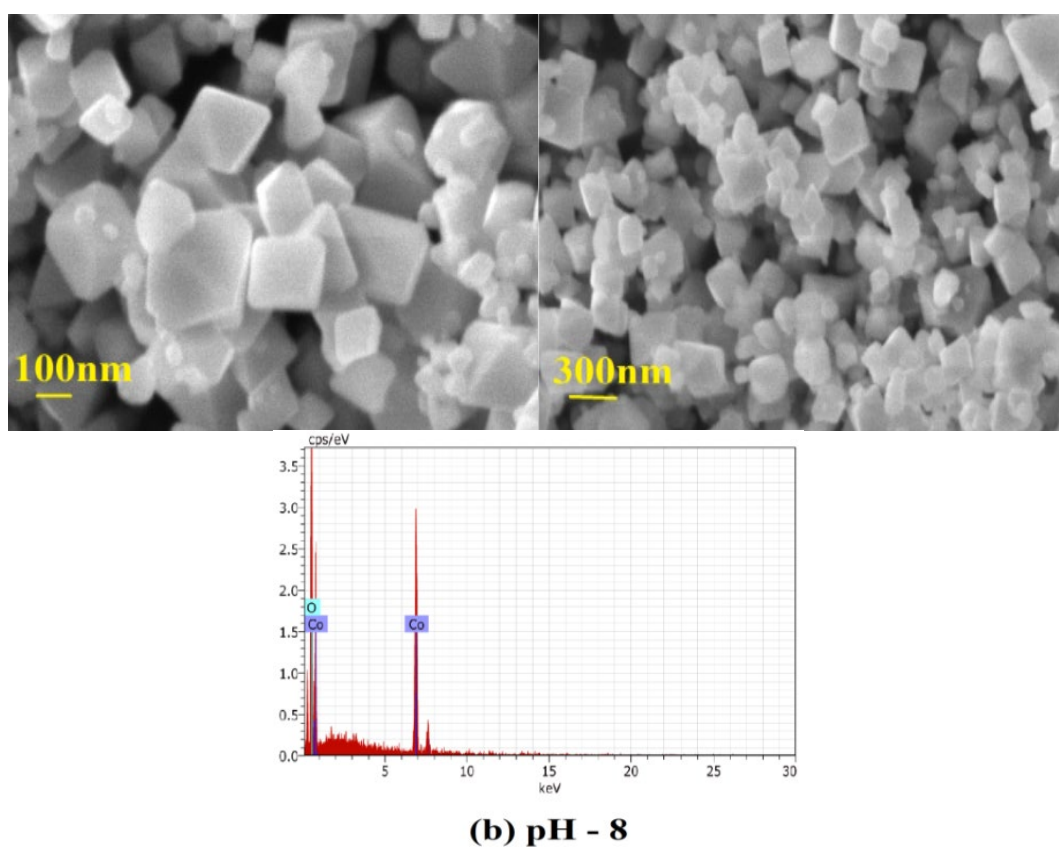
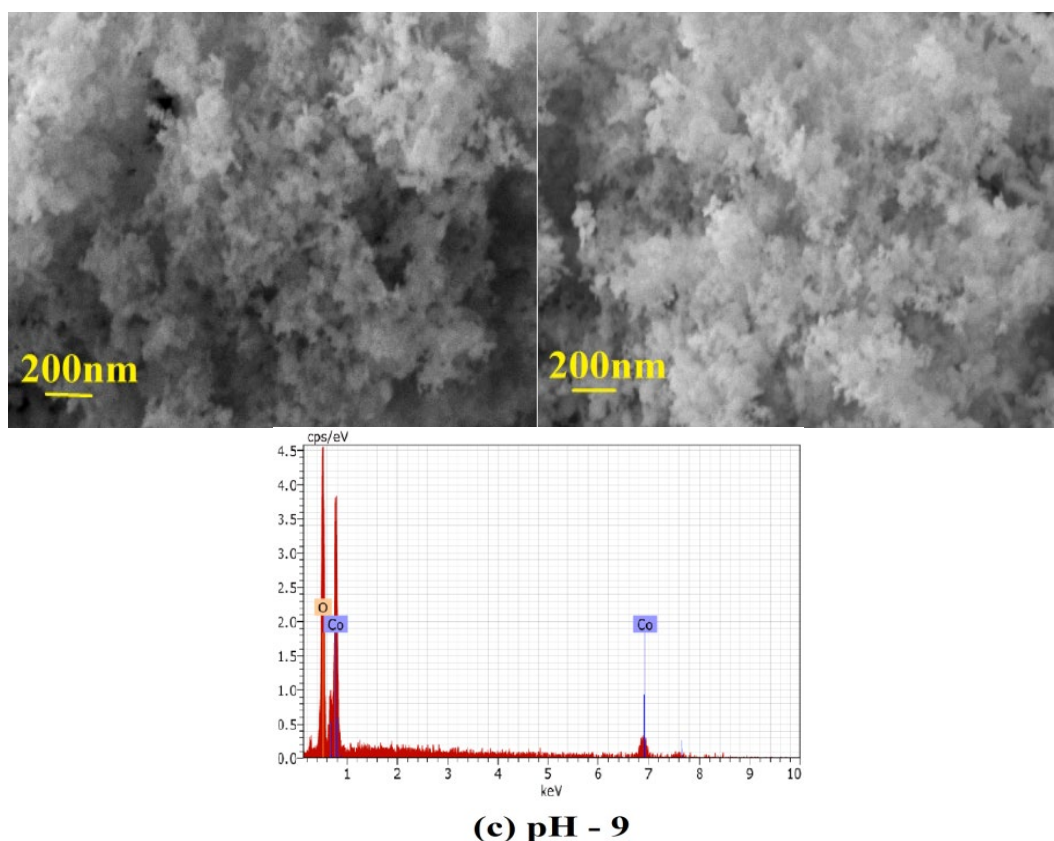*Fig. 4. (b) SEM Image of Co3O4 nanoparticles and EDX Spectrum of Co3O4 nanoparticles b=(pH=8.0).*

Fig. 4. (c) SEM Image of Co3O4 nanoparticles and EDX Spectrum of Co3O4 nanoparticles (pH=9.0).

3.3. Dielectric Studies

Dielectric studies are the essential technique to analyze electrical properties such as dielectric permittivity, AC conductivity, and the process involved in conducting materials. Further, it gives the details of how materials respond to applied electric fields. The various polarization techniques such as ionic, electronic, space charge and orientation polarization take place at different temperatures and frequencies. In order to carry out electrical measurements, the synthesized materials are formed into a pellet using a pelletizer. Silver coating is given on both sides of the sample which acts as an electrode. The dielectric measurements were carried out using the two-probe setup. The chamber used for the measurement was evacuated and filled with helium gas before the commencement of the measurements to avoid the adsorption of moisture on the surface of the sample.

3.3.1. Dielectric Constant

Dielectric studies give information about the grain boundary, transport characteristics, and charge storage capacity of synthesized samples. The variation of dielectric constant with frequency at various temperatures (40ºC to 250ºC) for the prepared Co_3O_4 is shown in Figure 5(a-c). The dielectric constant is higher at lower frequencies and decreases as frequency increases in all three pH levels which can be ascribed to the presence of space charge polarization in the grain boundaries [26,5]. A high dielectric constant at a low frequency corresponds to Maxwell–Wagner type of interfacial polarization [27]. On the other side, the dielectric constant decreases drastically as temperature increases in all pH levels. This arises due to the alignment of all dipoles in the same direction which gives more dipole moments as temperature increases [1].
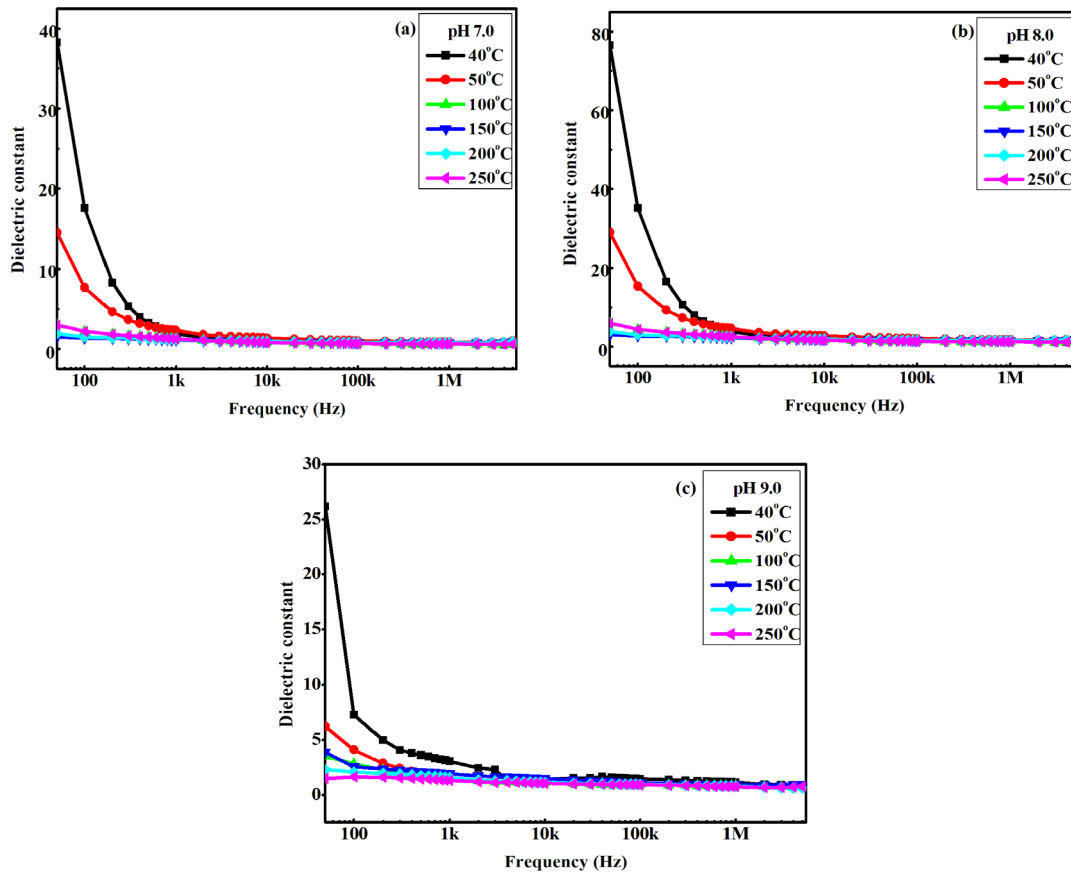
Fig. 5. (a) Dielectric Constant with frequency at pH (7.0) with various temperatures; (b) dielectric Constant with frequency at pH (8.0) with various temperatures; (c) dielectric constant for Co3O4 at pH (9.0) with different temperature.

3.3.2. Dielectric Loss

The frequency dependence of dielectric loss for Co_3O_4 at different temperatures is shown in Figure 6. (a, b & c). The dielectric loss is high at low-frequency regions and gradually decreases with increasing frequency in all three pH levels. The dielectric loss value increases at high-temperature pH levels region due to the thermal agitation of the atoms [28]. Thermal agitation of atoms increases the mobility of charge carriers and there increases the dielectric polarization, and hence at a high-temperature dielectric loss is more. Similarly at low temperatures, due to less thermal energy no thermal agitation of atoms gives a reduction in dielectric loss.
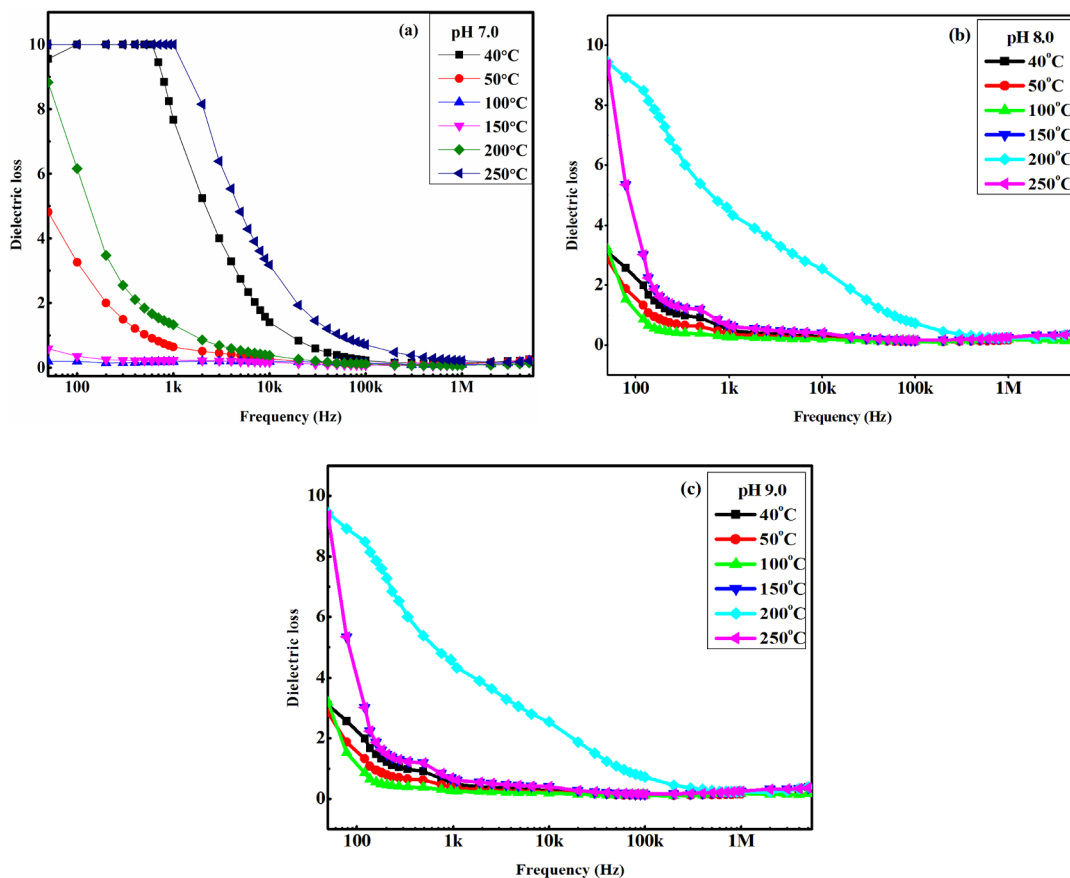
Fig. 6. (a) Dielectric losses for Co3O4at pH (7.0) with different temperatures; (b) Dielectric loss for Co3O4 at pH (8.0) with different temperatures; (c) Dielectric loss for Co3O4 at pH (9.0) with different temperatures.

3.3.3. Cole-Cole Plot

The Cole-Cole impedance plot is used to analyze the electrical properties of synthesized samples. It gives the information about grain and grain boundaries. This spectrum comprises two semicircles that attribute to the grain boundaries at low and high frequencies. Cole-Cole impedance plots of cobalt oxide nanoparticles at different temperatures for varying pH have been plotted as shown in Fig 7 (a-c). The Cole-Cole plot constitutes one major and one minor semi-circular curve, which represents the grain resistance and grain boundaries, features respectively [29-31]. Here, the small relaxation arcs at the low-frequency region accommodate the grain conduction and the major relaxation arcs at the high-frequency region correspond to the grain boundary conduction alone. The high-temperature semi-circle could result due to certain factors such as grain/ crystallite size, interstitial/vacancy defects, interface/grain boundary, stress-strain factor, or cell volume-fraction of the compounds [28]. The DC conductivity values were determined from the intersection point of the two semi-circles, where the conductivity and Z' values lowered for the increase in temperature as shown in Table 2.

3.3.4. Arrhenius Plot of Co_3O_4 Nanoparticles

Figure 8 shows the DC conductivity can be obtained from the Arrhenius equation, to calculate the activation energy. In general, the activation energy (Ea) corresponds to the position of trap energy levels below the conduction band. The activation energy is calculated from the slope of the Arrhenius Plot and it was found to be 0.4 eV, 0.45 eV, and 0.423 eV for samples at pH levels 7, 8, and 9 respectively. This variation in activation energy depends on the parameters like ionic radii, lattice parameter, grain boundary, surface atoms, and oxygen vacancy and carrier density [30, 32]. It is due to the presence of Co2+ / Co3+ ions in the materials [33]. The increase

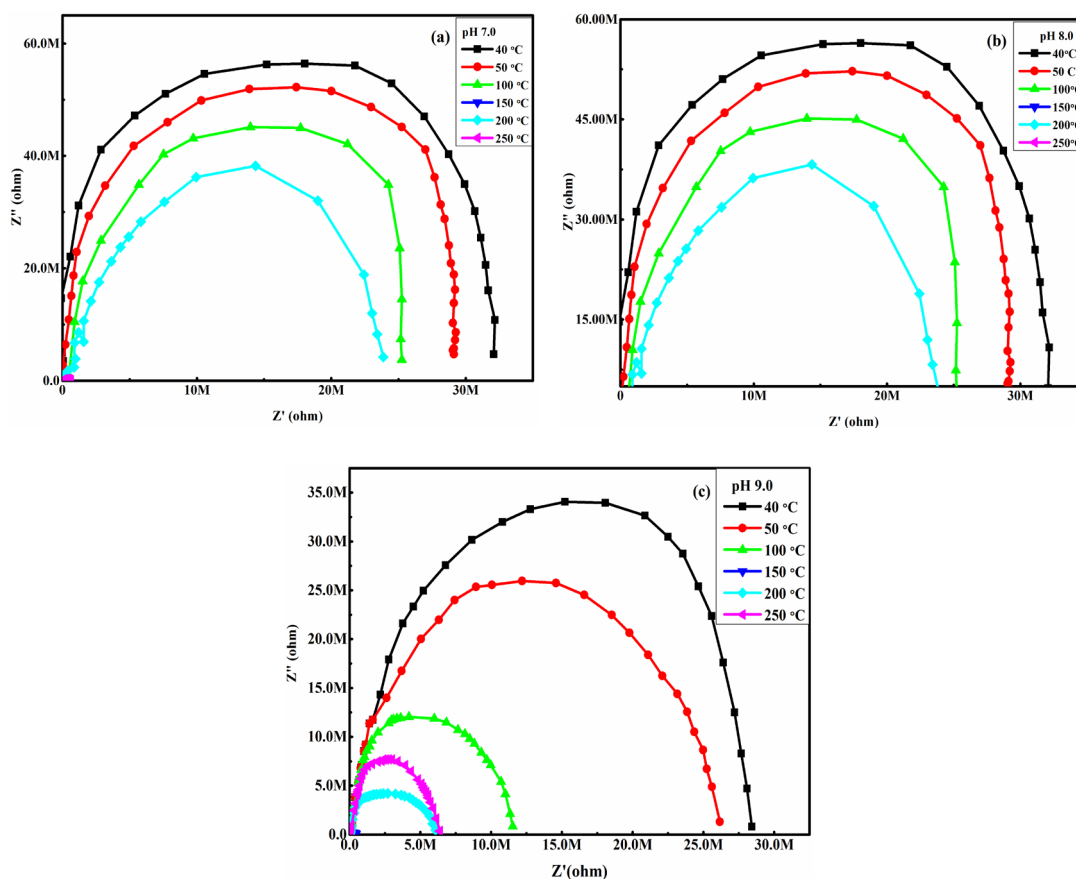in activation energy at pH level 8.0 gives an increase in conductivity which is confirmed in Table 2 [1].

Fig. 7. (a) Cole – Cole plot of Co3O4at pH 7.0 with different temperatures; (b) Cole – Cole plot of Co3O4 at pH 8.0 with different temperatures; (c) Cole – Cole plot of Co3O4 at pH 9.0 with different temperatures.

Table 2. DC conductivity of Cobalt Oxide Nanoparticles for different pH Level.

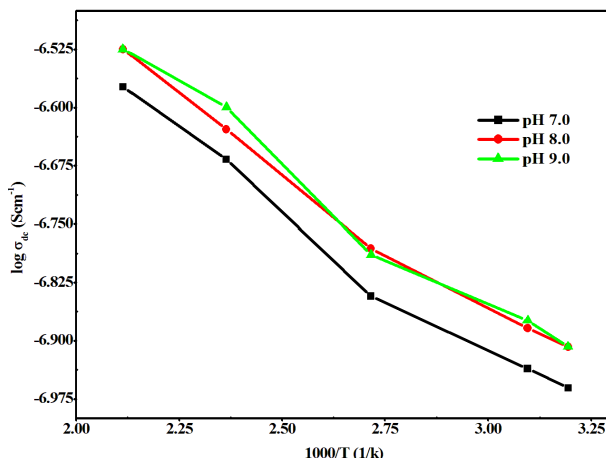| S.No	Temperature	DC conductivity (nS)		
		pH 7.0	pH 8.0	pH 9.0
1.	40	311.85	352.15	340.05
2.	50	342.74	378.11	364.20
3.	100	397.57	410.22	421.30
4.	150	397.92	498.31	549.84
5.	200	422.98	524.67	482.23
6.	250	610.96	626.91	524.67

Fig. 8. Arrhenius plot of Cobalt oxide nanomaterials with various pH values.

4. Conclusion

Co_3O_4 nanoparticles were synthesized by the Sol-Gel method by maintaining various pH levels. The prepared sample exhibited a cubic structure with a space group Fd3m. The crystallite size was estimated by Scherrer's formula and it was observed that the reduction in particle size with increase in pH levels. SEM micrographs confirm the pH levels of the solution play major roles in the shape of the synthesized particles. Elemental confirmation of the existence of cobalt and oxygen was done by EDX measurements. A high dielectric constant was observed at lower frequencies due to the space charge polarization effect. Cole- Cole impedance spectra represent the major relaxation arcs at high-frequency regions which attributes to the grain boundary conduction. The activation energy was found to be 0.4 eV, 0.45 eV, and 0.423 eV for samples pH 7, 8, and 9 respectively which makes synthesized samples appropriate materials in electronic applications. Finally, this research works confirms the impact of pH levels of synthesized sample on the morphology, dielectric, and impedance spectral behavior of cobalt oxide nanomaterials.

References

[1] Nisha J. Tharayila,, S. Sagarb,1, R. Raveendrana , A.V. Vaidyan, Physica: B. (2007): 399: 1-8; https://doi.org/10.1016/j.physb.2007.03.037

[2] Murthy S. Chavali & Maria P. Nikolova, SN Applied Science. (2009): 606 (1); https://doi.org/10.1007/s42452-019-0592-3

[3] Ji Yong Choi, Chan Kyu Lim, Bumjin Park, Minjun Kim, Aqil Jamal, and Hyunjoon Song, Journal of Materials Chemistry A. (2019): 1(3): 15068-15072; https://doi.org/10.1039/C9TA04323C

[4] O.M. Sousa, J.S. Lima, A.F. Lima, M.V. Lalic, Journal of Magnetism and Magnetic Materials. (2019): 484: 21-30; https://doi.org/10.1016/j.jmmm.2019.03.122

[5] H. Bindu Duvurua, S.K. Allab,c, S.K. Shawb, Sher Singh Meenad, Nidhi Guptae, B.B.V.S. Vara Prasadf, M.M. Kothawaleg, M.K. Kumara, N.K. Prasad, Ceramics International. (2019):45:16512-16520; https://doi.org/10.1016/j.ceramint.2019.05.185

[6] Moumita Ghosh, E. V. Sampathkumaran, and C.N.R. Rao, Chem. Mater. (2005):17:2348-2352; https://doi.org/10.1021/cm0478475

[7] C.S.S.V. Pradeep, S.K. Alla, A. Sharma, Arun B, M. Vasundhara, A.Gangwar, S.K. Sha, N.K. Prasad, Inorganic Chemistry Communications.(2022):142:109698; https://doi.org/10.1016/j.inoche.2022.109698

[8] G. Anandha Babu, G. Ravi, Y. Hayakawa, M. Kumaresavanji, Journal of Magnetism and

Magnetic Materials.(2015): 375:184-193; https://doi.org/10.1016/j.jmmm.2014.09.062

[9] Liying Zhang, Desheng Xue, Journal Of Materials Science Letters. (2002):21:1931- 1933; https://doi.org/10.1023/A:1021656529934

[10] Mohammad Kashif Uddin, Umair Baig, Journal of Cleaner Production. (2019): 211:1141-1153; https://doi.org/10.1016/j.jclepro.2018.11.232

[11] Ramany Revathy, Anoop A. Nair, Manoj Raama Varma, Kuzhichalil Peethambharan Surendran, Materials Science and Engineering: B Volume.(2021): 273:115453; https://doi.org/10.1016/j.mseb.2021.115453

[12 Muhammad Ramzan Saeed Ashraf Janjua, Open Chem.(2019):17:865-873; https://doi.org/10.1515/chem-2019-0100

[13] M E Andrade-Sanchez , M A Hernandez-Perez , G García-Pacheco and M Ortega-Avilés, Mater. Res. Express.(2021):8:025015; https://doi.org/10.1088/2053-1591/abe65a

[14] B. Vennela, D. Mangalaraj, N. Muthukumarasamy, S. Agilan, K.V. Hemalatha, Int. J. Electrochem. Sci.(2019):14:3535 – 3552; https://doi.org/10.20964/2019.04.40

[15] C. Indira Priyadharsini, G. Marimuthu T. Pazhanivel, P. M. Anbarasan, V. Aroulmoji V. Siva, L. Mohana, Journal of Sol-Gel Science and Technology. (2020):96:416-422; https://doi.org/10.1007/s10971-020-05393-x

[16] S. K. Alla, Hima Bindu Duvuru, S. K. Shaw, B. B. V. S. Vara Prasad, M. K. Kumar Sher Singh Meena Nidhi Gupta, N. K. Prasad, Journal of Materials Science: Materials in Electronics.(2019):30:20088-20098; https://doi.org/10.1007/s10854-019-02381-y

[17] M. Abdallah & R. Awad, Journal of Superconductivity and Novel Magnetism.(2019):33:1395-1404; https://doi.org/10.1007/s10948-019-05296-1

[18] Ghazaleh Allaedini and Abubakar Muhammad, Journal Of Nanostructure in Chemistry.(2013):3:77; https://doi.org/10.1186/2193-8865-3-77

[19] Lukasz Marciniak, Martyna Nowak, Anna Trojanowska, Bartosz Tylkowski and Renata Jastrzab, Materials.(2020):13:5444; https://doi.org/10.3390/ma13235444

[20] Abebe G. Habte, Fekadu Gashaw Hone, Francis B. Dejene, Physica B: Physics of Condensed Matter.(2019):580; https://doi.org/10.1016/j.physb.2019.411832

[21] Jianhua Zhang, Jiecheng Zheng, Yecheng Li, Yuqian Liu, Wentao Hao, Lingyan Lin,Yuanyuan Li, Jiancheng Song, Journal of Alloys and Compounds.(2018):779:255-260; https://doi.org/10.1016/j.jallcom.2018.11.244

[22] Jin Zhu, Wenbin Li, Mao Zhu, Wei Zhang, Wencheng Niu, and Guohua Liu, AIP Advances.(2014):4:031338; https://doi.org/10.1063/1.4869615

[23] Fatma Meydaneri Tezela, İshak Afşin Kariper, Materials Research. (2017): 20(6): 1563-1570; https://doi.org/10.1590/1980-5373-mr-2017-0319

[24] MasoudSalavati- Niasari, AfsanehKhansariC. R. Chimine.(2014):17(4):352-358; https://doi.org/10.1016/j.crci.2013.01.023

[25] Masumeh Galini, Mehdi Salehi, Mahdi Behzad, Structural, J Nanostruct.(2018):8(4):391-403.

[26] G. Murtazaa, S. H. Bukharia, J. Ahmadb, M. T. Jamilb, U. Nissarb, F. Mazharc, A. Hakeem, Digest journal of nanomaterials and biostructures.(2018):13(2):337-344.

[27] Ch. Rayssi S. El.Kossia, J. Dhahri and K. Khirouni, RSC Adv. (2018):8:17139-17150; https://doi.org/10.1039/C8RA00794B

[28] Laurel Simon Lobo, S. Kalinathan, A. Ruban Kumar, Superlattices and Microstractures.(2015):88:116-126; https://doi.org/10.1016/j.spmi.2015.09.010

[29] W. Chen, W. Zhu, Ferroelectrics - Material Aspects, 2010; https://doi.org/10.5772/10646

[30] M.M. Yao, Z.H. Hu, Z.J. Xu, Y.F. Liu, P.P. Liu, Q. Zhang, Elctrochim. Acta.(2015): 158:96-104; https://doi.org/10.1016/j.electacta.2014.12.058

[31] Raja Yasir Mehmood, M. F. Afsar, A. Jamil, S. Fareed, F. Siddique, M. H. Bhatti, M. Ali & M. A. Rafiq, Journal of Taibah University for Science.(2021):15(1):1144-1155; https://doi.org/10.1080/16583655.2021.2011595

[32] M. Manickam, V. Ponnuswamy, C. Sankar, R. Suresh, R. Mariappan, and J. Chandrasekaran, Int. J. Thin. Fil. Sci. Tec.(2016):5(3):155-161; https://doi.org/10.18576/ijtfst/050302
[33] Rao, K. V, Smakula, A, Journal of Applied Physics,(1965):36(6):2031-2038; https://doi.org/10.1063/1.1714397